Inorganic Chemistry

Article

pubs.acs.org/IC

Argentophilicity as Essential Driving Force for a Dynamic Cation−Cation Host−Guest System: $[Ag(acetonitrile)_2]^+ \subset [Ag_2(bis\text{-}NHC)_2]^{2+}$ (NHC = N-Heterocyclic Carbene)

Alba Vellé,[†] Andrea Cebollada,[†] Manuel Iglesias, and Pablo J. Sanz Miguel*

Departamento de Química Inorgánica, Instituto de Síntesis Química y Catálisis Homogénea (ISQCH), Universidad de Zaragoza-CSIC, 50009 Zaragoza, Spain

Supporting Information

ABSTRACT: A cationic $[Ag_2(bis\text{-}NHC)_2]^{2+}$ system behaves as an excellent host for Ag^+. In the solid-state variation, Ag···Ag are the only bonding interactions between host and guest, overcoming their inherent electrostatic repulsion. It represents a clear example of ligand-unsupported ("pure") argentophilicity. In solution, we also found evidence for this kind of Ag···Ag approximation, which might be recognized as an initial step of transmetalation mechanisms involving formally closed-shell metal centers as transferring agents.

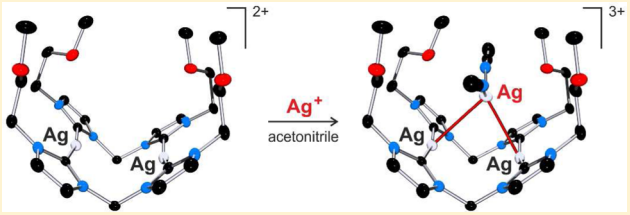

1. INTRODUCTION

Fine-tuning of host−guest systems encompasses all fields in classical and modern chemistry. Such associates exist in nature and artificial systems, involving discrete and polymeric hosts and guests, in one, two, and three dimensions, and of cationic, neutral, and anionic nature. In the stabilization of guest molecules within adequate host cavities, a significant role is played by noncovalent secondary interactions, such anion−π, lone pair−π, hydrogen bonding, electrostatics, hydrophobicity, or metallophilicity. Some advanced host−guest applications involve processes in nanoporous materials,[1] molecular encapsulation,[2] catalysis,[3] biological signaling,[4] or drug delivery,[5] among others. Our interest resides in sophisticated metal−ligand constructs with the ability of capturing small molecules,[6] or interacting with DNA,[7] and in metallophilic bonding approaches (Ag···Ag and Ag···Pt).[8]

Within this frame, among modern ligands utilized by chemists, probably the host−guest chemistry supported by NHC complexes remains the most unexplored.[9] It is well-known that NHC ligands behave as strong σ-donor entities in terms of stabilization of metal complexes. They confer strength to the C−M bonds, enabling the availability of rare high oxidation states of transition metals, especially if two or more NHC ligands are implied. This principle of electron enrichment affects the metal properties, being usually exploited in catalytic strategies. In fact, it seems to be reasonable that metallophilicity in such situations could be likewise altered. This connects with the fact that Ag(I)−NHC complexes are widely employed as transfer agents,[10] with transmetalation mechanisms relatively unexplored.[11]

Here, we report on the outstanding case of a conformationaly dynamic cationic complex, $[Ag_2(bis\text{-}NHC)_2]^{2+}$, which acts as a host in solution and in the solid state for cationic $[Ag(acetonitrile)_2]^+$ guests, with silver−silver interactions being the only "glue" between cations. This work represents a clear evidence in the solid state of ligand-unsupported argentophilicity.[13] As NHC ligand, we selected methylenebis(*N*-2-methoxyethyl)-imidazole-2-ylidene, bisMeOEtIm, which has demonstrated to tune highly selective catalytic reactions,[12] to study the interesting behavior of the Ag species previous to the transmetalation step. The precursor, $[H_2bisMeOEtIm]I_2$ (**1**),[12a] was isolated as crystalline material (Supporting Information). A solution of **1** in acetonitrile was treated with $AgNO_3$ in order to achieve anion exchange, and, subsequently, with Ag_2O, yielding $[Ag_2(bisMeOEtIm)_2](NO_3)_2$ (**2**).

2. EXPERIMENTAL SECTION

Materials and Methods. All reagents were of commercial origin and used as received. NMR spectra were recorded on a Bruker Avance 300 MHz or a Bruker ARX 300 MHz instruments. Chemical shifts (in parts per million) are referenced to residual solvent peaks. High-resolution electrospray mass spectra (HRMS) were acquired using a MicroTOF-Q hybrid quadrupole time-of-flight spectrometer (Bruker Daltonics, Bremen, Germany). C, H, and N analyses were carried out in a PerkinElmer 2400 CHNS/O analyzer.

$[H_2bisMeOEtIm]I_2$ (1). Synthesis of compound **1** was carried out with slight modifications of the reported method.[12a] Anal. Calcd for $C_{13}H_{22}I_2N_4O_2$: C, 30.02; H, 4.26; N: 10.77. Found: C, 30.01; H, 4.40; N: 11.05. HRMS (electrospray, m/z): calcd. for $C_{13}H_{21}N_4O_2$ [**1** − H^+]$^+$: 265.1659. Found: 265.1642.

$[Ag_2(bisMeOEtIm)_2](NO_3)_2$ (2). A solution of **1** (88.3 mg, 0.17 mmol) and $AgNO_3$ (57.7 mg, 0.34 mmol) in 20 mL of acetonitrile was stirred at room temperature for 12 h with daylight excluded. The yellow precipitate was removed by filtration, and Ag_2O (78.7 mg, 0.34 mmol) was added to the filtrate. The resultant solution was then stirred for 1 day at room temperature in the dark, and the undissolved

Received: July 21, 2014
Published: September 16, 2014

   dx.doi.org/10.1021/ic501715h | *Inorg. Chem.* 2014, 53, 10654−10659

excess of Ag_2O was filtered off. The filtrate was concentrated to a small volume and kept at room temperature. A white precipitate was immediately obtained and promptly turned into oil. Colorless crystals were isolated by slow diffusion of diethyl ether over a solution of **2** in acetonitrile. Yield: 84% (62.8 mg). ^{1}H NMR (CD_3CN, δ ppm, 300 MHz, 0.023 mol L^{-1}): 7.63 (d, 4H, J_{H-H} = 1.9; H5im), 7.31 (d, 4H, J_{H-H} = 1.9; H4im), 6.56 (s, 4H, CH_2 bridge), 4.34−4.26 (m, 8H; CH_2(N)), 3.70−3.62 (m, 8H; CH_2(O)), 3.23 (s, 12H; CH_3). ^{13}C NMR (CD_3CN, δ ppm, 70 MHz, 0.023 mol L^{-1}): 182.9 (s; C2im), 124.3 (s; C4im), 122.4 (s; C5im), 72.4 (s; CH_2(O)), 65.1 (s; CH_2 bridge), 59.1 (s; CH_3), 52.9 (s; CH_2(N)). HRMS (electrospray, m/z): calcd. for $C_{26}H_{40}Ag_2N_8O_4$ [**2** − $(NO_3)_2$]$^{2+}$: 371.0632. Found: 371.0608. Anal. Calcd for $C_{26}H_{40}Ag_2N_{10}O_{10}$: C, 35.96; H, 4.64; N: 16.13. Found: C, 35.75; H, 4.65; N: 16.14.

[Ag(CH$_3$CN)$_2$⊂Ag$_2$(bisMeOEtIm)$_2$](NO$_3$)(BF$_4$)$_2$ (3). An excess of $AgNO_3$ and $LiBF_4$ were added to a solution of **2** in acetonitrile, and the resulting solution was kept at 4 °C. Then, diethyl ether was slowly diffused into the solution. Colorless crystals of **3** were picked up under the microscope and analyzed by X-ray crystallography. The nitrate variation of **3** could not be isolated by crystallization. ^{1}H NMR (CD_3CN, δ ppm, 300 MHz, 0.023 mol L^{-1}): 7.63 (d, 4H, J_{H-H} = 1.9; H5im), 7.31 (d, 4H, J_{H-H} = 1.9; H4im), 6.56 (s, 4H, CH_2 bridge), 4.34−4.27 (m, 8H; CH_2(N)), 3.69−3.62 (m, 8H; CH_2(O)), 3.23 (s, 12H; CH_3). ^{13}C NMR (CD_3CN, δ ppm, 70 MHz, 0.023 mol L^{-1}): 182.8 (s; C2im), 124.3 (s; C4im), 122.5 (s; C5im), 72.3 (s; CH_2(O)), 65.1 (s; CH_2 bridge), 59.1 (s; CH_3), 52.9 (s; CH_2(N)).

X-ray Diffraction Studies. Data collection for compounds **1**, **2**, and **3** were recorded at 100 K on an APEX-II diffractometer equipped with an area detector and graphite monochromated Mo Kα radiation (0.71073 Å). Data reduction of the diffraction images was performed using the APEX2 software.[14] All the structures were solved by direct methods and refined by full-matrix least-squares methods based on F^2 using the SHELXL-97 software.[15] Non-hydrogen atoms were refined anisotropically. Hydrogen atoms were positioned geometrically in idealized positions and refined with isotropic displacement parameters according to the riding model. All distance and angle calculations were performed using the SHELXL-97 and WinGX programs.[15,16]

Crystal Data for ***1****:* [$C_{13}H_{22}I_2N_4O_2$], monoclinic, $C2/c$, a = 26.864(3) Å, b = 4.9895(5) Å, c = 14.2758(13) Å, β = 103.4570(10)°, Z = 4, M_r = 520.15 g mol^{-1}, V = 1861.0(3) Å^3, D_{calcd} = 1.857 g cm^{-3}, λ(Mo Kα) = 0.71073 Å, T = 100 K, μ = 3.389 mm^{-1}, 10 981 reflections collected, 1931 unique (R_{int} = 0.0449), 1626 observed, $R1(F_o)$ = 0.0419 [$I > 2\sigma(I)$], $wR2$ (F_o^2) = 0.1258 (all data), GOF = 1.060. CCDC 984992.

Crystal Data for ***2****:* [$C_{26}H_{40}Ag_2N_{10}O_{10}$], triclinic, $P\bar{1}$, a = 12.7368(7) Å, b = 12.9169(7) Å, c = 13.2485(13) Å, α = 96.1050(10)°, β = 111.5210(10)°, γ = 115.6680(10)°, Z = 2, M_r = 868.42 g mol^{-1}, V = 1733.7(2) Å^3, D_{calcd} = 1.664 g cm^{-3}, λ(Mo Kα) = 0.71073 Å, T = 100 K, μ = 1.196 mm^{-1}, 28 456 reflections collected, 8169 unique (R_{int} = 0.0461), 7005 observed, $R1(F_o)$ = 0.0369 [$I > 2\sigma(I)$], $wR2(F_o^2)$ = 0.1090 (all data), GOF = 1.058. CCDC 984993.

Crystal Data for ***3****:* [$C_{30}H_{46}Ag_3B_2F_8N_{11}O_7$], triclinic, $P\bar{1}$, a = 10.8610(5) Å, b = 13.4839(6) Å, c = 15.6841(7) Å, α = 95.8020(10)°, β = 103.7650(10)°, γ = 110.3730(10)°, Z = 2, M_r = 1170.01 g mol^{-1}, V = 2048.28(16) Å^3, D_{calcd} = 1.897 g cm^{-3}, λ(Mo Kα) = 0.71073 Å, T = 100 K, μ = 1.516 mm^{-1}, 36 813 reflections collected, 9712 unique (R_{int} = 0.0271), 8645 observed, $R1(F_o)$ = 0.0363 [$I > 2\sigma(I)$], $wR2(F_o^2)$ = 0.0925 (all data), GOF = 1.014. CCDC 984994.

Quantum Chemical Calculations. Density functional theory calculations were performed to estimate the binding energies of cations of **2** and **3** from (i) the crystallographic model, and (ii) after completing geometry optimizations. We used M06[17] and B3LYP[18] functionals in the gas phase and with acetonitrile as solvent, through the polarizable continuum method (smd).[19] Silver was represented by the relativistic effective core potential from the Stuttgart group,[20] whereas the basis sets used for C, N, O, and H were 6-311+G(d,p). All calculations were performed through the Gaussian09 software.[21] Coordinates are given in the Supporting Information.

3. RESULTS AND DISCUSSION

Cation **2** has the shape of an open-book (U conformer), with a pair of ligands of **1** cross-linked via their C2 sites by silver ions and a dihedral angle of 73.38(7)° (Figure 1). Silver

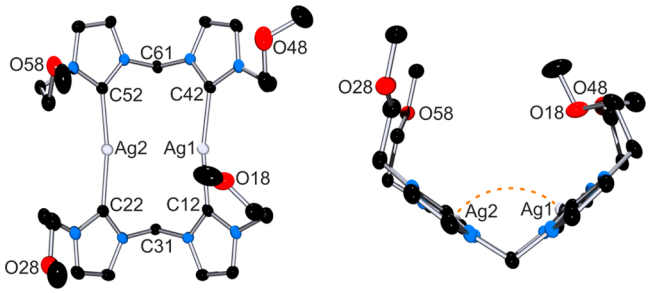

Figure 1. Upper (left) and side (right) views of complex **2**, detailing the dihedral angle of 73.38(7)° (dashed line).

coordination at the C2 sites affects the geometry of the imidazolium rings, and, in particular, the N1−C2−N3 angle, which is diminished from 108.0(5)° (free ligand **1**), to nearly 103.6(3)° in **2**. The Ag1−Ag2 distance (3.4512(5) Å) slightly exceeds 2 times the van der Waals radius of silver (2 × 1.72 = 3.44 Å). Both C−Ag−C angles are directed in such a way that Ag1 and Ag2 come close to each other. Thus, considering the absence of additional remarkable interactions of the silver ions with surrounding atoms (only the O18 ether atom is relatively close, 3.087(3) Å, to the interacting sphere of Ag1), and despite this long Ag1−Ag2 distance, the existence of silver−silver interactions should not be fully discarded here. The ^{1}H NMR spectrum of **2** displays an analogous pattern as that of **1**, with the expected resonance divergences due to the metal coordination. A significant difference concerns the resonance of the $-CH_2-$ bridges between imidazolium rings, which appears as a broad signal. This fact strongly suggested [Ag_2(bisMeOEtIm)$_2$]$^{2+}$ (**2**) to display conformational flexibility by rotation about the methylene bridges. To illustrate this behavior, we performed DFT calculations in order to optimize and compare both possible conformers, namely, the U (open-book) and Z (chair) forms (Figure 2). The U conformer resulted to be more stable than the Z form by 6.1 kcal mol^{-1}.

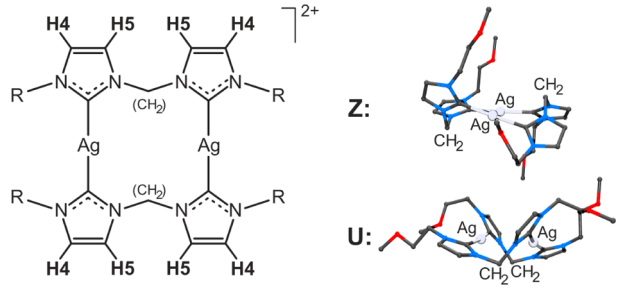

Figure 2. Assignment of NMR resonances, and view of the optimized U (open-book) and the Z (chair) forms of **2**.

A ^{1}H NMR temperature-dependent study was carried out with the aim of corroborating this premise (Figure 3). Regarding the proton resonances of **2** at the different temperatures, the following conclusions can be drawn: First, by a gradual warming up of the sample, the CH_2 signal moderately shifts to the lower field and becomes sharper. This implies an increase of the conformational Z ⇋ U conversion

dx.doi.org/10.1021/ic501715h | Inorg. Chem. 2014, 53, 10654−10659

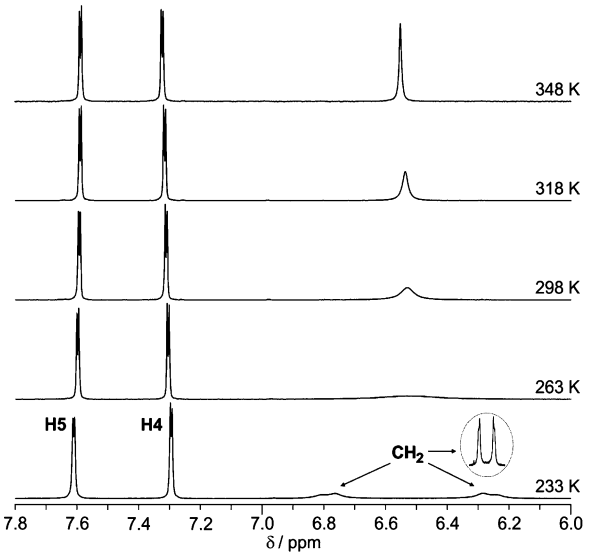

Figure 3. Temperature-dependent ^{1}H NMR spectra of **2** (0.023 M) in acetonitrile (see also the Supporting Information), with isolation of the U conformer (inset).

rate. Second, by decreasing the temperature, full conversion into a unique conformer (U) is realized. The spectrum at 233 K shows how the methylene protons of the ethyl bridges split into two signals due to the loss of chemical equivalency because of the fixed environment. They construct an AB system, in which both methylene protons pointing toward the silver ions are centered at 6.78 ppm, whereas their geminal partners appear at 6.25 ppm. At 233 K, the geminal coupling between both CH_2 resonances is discernible (J_{H-H} = 12 Hz). Conversion rate constants were estimated from NMR line-shape analysis, ranging from 52.9 s^{-1} (233 K) to 1.35 × 10^5 s^{-1} (348 K). The enthalpy ($\Delta H^{\ddagger}$) and entropy of activation ($\Delta S^{\ddagger}$) were found to be 8.4 ± 0.2 kcal mol^{-1} and −13.9 ± 0.7 cal mol^{-1} K^{-1} (Eyring analysis).

The dynamic behavior of **2** was also evidenced in concentration-dependent ^{1}H NMR measurements (Figure 4). From this study, we can confirm an aggregation propensity between cations of **2** in solution along with an increase of the conformational Z ⇋ U conversion in higher concentrated samples. Both conclusions are supported on (i) the shifts of the

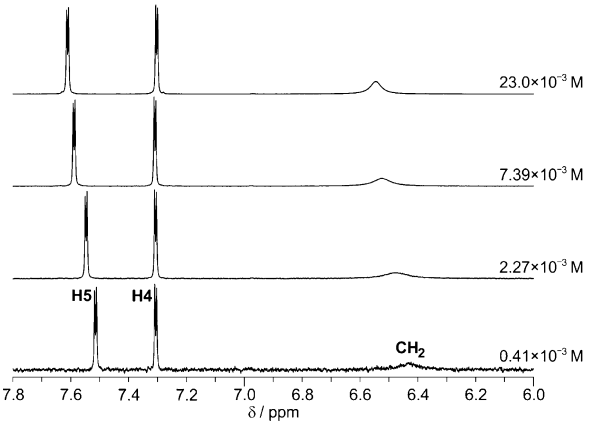

Figure 4. Downfield fragments of several ^{1}H NMR spectra of **2** in acetonitrile at different concentrations (see also the Supporting Information).

signals corresponding to H5 ($\Delta\delta$ = 0.10 ppm) and CH_2 ($\Delta\delta$ = 0.12 ppm), which are strongly affected, and (ii) the broadening of the proton signals of the methylene bridge at lower concentrations. Curiously, the faster Z ⇋ U conversion of **2** at higher concentrations seems not to hinder the intermolecular aggregation at the NMR scale.

The hydrodynamic radii (r_H) at different concentrations of cation **2** were estimated from ^{1}H DOSY NMR experiments following the Stokes−Einstein equation ($D = kT/6\pi\eta r_H$). The average r_H was found to be 5.32 Å for the concentrated solution (0.023 M), whereas the value for the diluted sample (4 × 10^{-3} M) was 4.67 Å. This result also supports the aggregation tendency of cations **2** in solution.

In order to test the affinity of **2** toward additional silver ions, increasing amounts of $AgNO_3$ were added to a solution of **2** in acetonitrile and monitored on ^{1}H NMR (Figure 5).

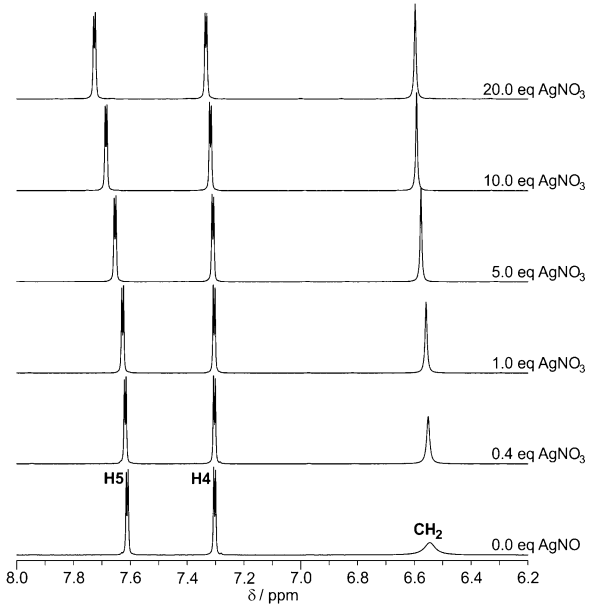

Figure 5. Sections of ^{1}H NMR spectra of compound **2** in acetonitrile (0.023 M) with increasing amounts of Ag^+ ($AgNO_3$) added (Supporting Information).

Interestingly, if compared to the concentration-dependent study, parallel conclusions can be extracted: (i) Aggregation in solution is observed between $[Ag(acetonitrile)_2]^+$ and the cations of **2**, which affects the chemical shifts of H5 ($\Delta\delta$ = 0.11 ppm) and CH_2 ($\Delta\delta$ = 0.05 ppm) at high concentrations of Ag^+ ions (20 equiv of $AgNO_3$). Here, interactions exclusively between cations of **2** cannot be discarded. (ii) A prominent increase of the conformational Z ⇋ U conversion in samples even with a minor presence of Ag^+ ions is deduced from these data. Analogously, addition of Ag^+ to the diluted solution (0.4 × 10^{-3} M) of **2** in CD_3CN also induced a notable downfield shift of the H5 and CH_2−bridge signals (Supporting Information). Thus, ^{1}H NMR spectroscopy confirms the existence in solution of aggregates based on argentophilic interactions (Ag^+···**2** and **2**···**2**), and that the conversion between the Z and the U forms is facilitated by increasing argentophilic interactions. A quantitative evaluation of these experiments proved impossible because of the random formation in solution of multiple species and interactions.

The acetonitrile residual peak signal is strongly affected by the presence of Ag^+, undergoing a notable low-field shift

dx.doi.org/10.1021/ic501715h | Inorg. Chem. 2014, 53, 10654−10659

provoked by rapid formation of $[Ag(acetonitrile)_2]^+$ and by the lability of the silver ions in CD_3CN (rapid ligand exchange). Thus, the presence of an internal standard is necessary when a moderately large amount of Ag^+ ions is present (CH_2Cl_2 in our case).

All of our attempts to crystallize the title host–guest system as its nitrate salt had failed. Only after addition of $LiBF_4$ to a solution mixture of **2** and $AgNO_3$ could suitable crystals for X-ray analysis be isolated as $[Ag(CH_3CN)_2{\subset}Ag_2(bisMeOEtIm)_2](NO_3)(BF_4)_2$ (**3**). Figure 6 evidences the most

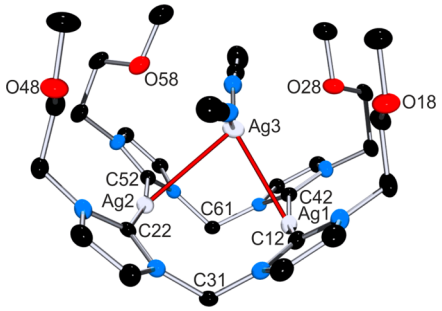

Figure 6. Side view of the host–guest system of **3** with atom numbering scheme.

remarkable feature of **3**: the presence of a cationic $[Ag(CH_3CN)_2]^+$ guest in the molecular cavity of the $[Ag_2(bisMeOEtIm)_2]^{2+}$ host. This is, to our best knowledge, the first crystallographic evidence of ligand-unsupported argentophilicity, which overcomes the Coulombic repulsion.

Incorporation of the $[Ag(CH_3CN)_2]^+$ guest is realized without a significant modification of the $[Ag_2(bisMeOEtIm)_2]^{2+}$ skeleton, as evidenced by the X-ray crystallography. Some resultant structural features of **3** are: The dihedral angle is 72.71(8)°, and Ag–C distances range from 2.118(3) Å (Ag1–C42) to 2.086(3) Å (Ag2–C22). Geometrical distortion of the imidazolium rings by silver coordination is likewise similar (N1–Ag–N3, av. 103.8(3)°). A plausible difference is observed in the Ag1–Ag2 distance (3.6587(4) Å), which is ca. 0.21 Å longer than that of cation **2**. This relatively small alteration almost certainly hinders argentophilic interactions between both silver centers in **3**. Some structural variations are observed regarding the positioning of the ether side arms, which are accommodated differently in the crystal packing.

The Ag–Ag host–guest distances are relatively short: 2.8231(4) Å (Ag1–Ag3) and 2.9952(4) Å (Ag2–Ag3). It strongly suggests the existence of metal–metal interactions between the silver guest Ag3 and both silver hosting atoms, especially between Ag1 and Ag3. The lopsided accommodation of the $[Ag(CH_3CN)_2]^+$ cation brings the potential interaction sphere of Ag3 closer to a C2 carbene atom (Ag3–C42, 2.735(3) Å; Ag3–C52, 2.940(3) Å), and to two oxygen ethers (Ag3–O48, 2.780(3) Å; Ag3–O58, 2.895(3) Å). The internal N71–Ag3–N81 angle (137.69(11)°) of the $[Ag(CH_3CN)_2]^+$ guest is far from linearity, which denotes a pronounced distortion of the linear silver coordination geometry toward tetrahedral, considering Ag1 and Ag2 to occupy the remaining coordination sites. As no H bonding, π–π stacking, or anion–π interactions are observed within the crystal lattice of **3**, common packing effects are discarded to be responsible for the proximity between silver atoms.

DFT calculations were carried out with **2** and **3** in order to understand their electronic properties and the stabilization phenomenon observed in **3**. We estimated the binding energies of these systems from the crystallographic model, and after completing geometry optimizations. For that, the M06 and B3LYP functionals in the gas phase, and with water and acetonitrile in a polarizable continuum model were used, resulting in different outcomes. Our initial aim was to evaluate the argentophilic interactions found in **3**, as a single $[Ag(CH_3CN)_2{\subset}Ag_2(bisMeOEtIm)_2]^{3+}$ host–guest entity, and its relationship with each fragment: $[Ag_2(bisMeOEtIm)_2]^{2+}$ and $[Ag(CH_3CN)_2]^+$. Calculations with crystal coordinates of **3** without further optimization revealed that the relative stabilization energy of the host–guest entity is essentially attributed to argentophilic interactions, which could be estimated from the following equation: $\Delta E(\mathbf{3}) = E(\text{host–guest } \mathbf{3}) - E(\text{host } \mathbf{3}) - E(\text{guest } \mathbf{3})$. There, the stabilization energy "ΔE" results from the difference between the energy of the host–guest entity, "E(host–guest **3**)", and the energy of the two $[Ag_2(bisMeOEtIm)_2]^{2+}$ "E(host **3**)" and $[Ag(CH_3CN)_2]^+$ "E(guest **3**)" fragments. As a result, we present the host–guest system to be stabilized by 35.5 kcal mol^{-1} (M06, smd, CH_3CN).

Analogous calculations revealed cation **2** and host **3** to be approximately isoenergetic, with a difference of 0.2 kcal mol^{-1} (ΔE(**2** – host **3**)): E(**2**), −128 3794.1 kcal mol^{-1}; E(host **3**), −128 3794.3 kcal mol^{-1}. Thus, in terms of relative energy, we can assert that the presence of the Ag^+ guest does not significantly affect the geometrical interactions of the $[Ag_2(bisMeOEtIm)_2]^{2+}$ core. For comparison, optimizations of the molecular geometry of host–guest **3** were completed (Supporting Information). There are three important points to take into account: (i) The optimized geometries stabilized the host–guest system **3** by 37.6 kcal mol^{-1}; (ii) the energy of the optimized cations is considerably lower in comparison to the analogous crystal coordinates (e.g., ΔE(opt. **3** – nonopt. **3**), −258.6 kcal mol^{-1}); and (iii) the existence of molecular orbitals involving Ag(host)···Ag(guest) interactions is patent (Figure 7), but not that of Ag(host)···Ag(host) contacts.

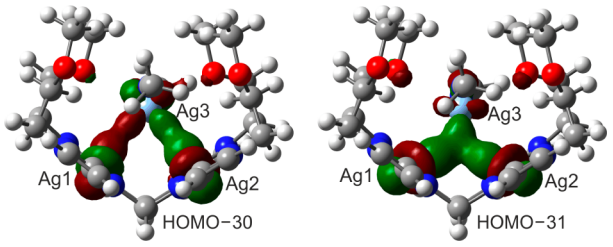

Figure 7. Detailed view of the Ag···Ag binding orbitals in the optimized geometry of **3**.

Although the optimized DFT stabilization energy of **3** does not give a significant difference with the nonoptimized one (ΔE = 2.1 kcal mol^{-1}), molecular arrangement, intramolecular interactions, and relative energies between fragments differ substantially. Two notable deviations could alter the nature of the Ag···Ag contacts: (i) The Ag1–Ag2 lengths are ca. 0.3 Å shorter in the optimized geometries, and to a lesser degree, distances between the silver guest (Ag3) atom and both silver hosts show an identical tendency. (ii) The ether functions lie considerably closer (ca. 0.2 Å) to Ag3 in the optimized structure. Thus, although isoenergetic, silver interactions inherent to the optimized and crystal models differ pronouncedly, especially those concerning the Ag···Ag

dx.doi.org/10.1021/ic501715h | Inorg. Chem. 2014, 53, 10654–10659

approaches, and, therefore, owing to the lack of a better theoretical model, we assume this study to be merely qualitative.

4. CONCLUSIONS

In summary, cation $[Ag_2(bisMeOEtIm)_2]^{2+}$ (**2**) exhibits a notable intermolecular aggregation tendency in solution based on Ag···Ag interactions. This is detectable by ^{1}H NMR spectroscopy even at low concentrations. Conversion between conformers (Z and U) of **2** is facilitated by an increase of the temperature, as well as by local argentophilicity. In the presence of Ag^+ ions, **2** has a remarkable dynamic interacting pattern, increasing its conformational flexibility and still allowing for argentophilic contacts (Ag^+···**2** and **2**···**2**). Crystals of cation **2** act as an excellent host for silver ions, $\{[Ag(acetonitrile)_2]\subset[Ag_2(bis\text{-}NHC)_2]\}^{3+}$ (**3**), representing a rare case of cation−cation host−guest entity. The argentophilicity found in this system was strong enough to overcome the inherent electrostatic repulsion between both positively charged fragments, enabling the stabilization of the host−guest system without ligand-supported assistance. Finally, we could not quantitatively evaluate the nature of Ag···Ag contacts due to the lack of an appropriate theoretical model. This kind of unsupported intermetallic approach in solution may be relevant for understanding the controversial transmetalation mechanisms, as most of them occur with formally closed-shell metal centers as transferring agents.

■ ASSOCIATED CONTENT

Ⓢ Supporting Information

Structural details, NMR measurements and simulations, DFT calculations, X-ray diffraction records [CCDC-984992 (**1**), 984993 (**2**), and 984994 (**3**)], and ESI-MS data are given in the Supporting Information. This material is available free of charge via the Internet at http://pubs.acs.org.

■ AUTHOR INFORMATION

Corresponding Author

*E-mail: pablo.sanz@unizar.es (P.J.S.M.).

Author Contributions

†These authors contributed equally.

Notes

The authors declare no competing financial interest.

■ ACKNOWLEDGMENTS

Financial support from the Spanish Ministerio de Economía y Competitividad ("Ramón y Cajal" program (P.J.S.M.) and CTQ2011-27593) is gratefully acknowledged.

■ REFERENCES

(1) See, e.g.: (a) Laeri, F., Schüth, F., Simon, U., Wark, M., Eds. *Host-Guest-Systems Based on Nanoporous Crystals*; Wiley-VCH: Weinheim, 2005. (b) Inokuma, Y.; Yoshioka, S.; Ariyoshi, J.; Arai, T.; Hitora, Y.; Takada, K.; Matsunaga, S.; Rissanen, K.; Fujita, M. *Nature* **2013**, *495*, 461−466. (c) Fujita, D.; Suzuki, K.; Sato, S.; Yagi-Utsumi, M.; Yamaguchi, Y.; Mizuno, N.; Kumasaka, T.; Takata, M.; Noda, M.; Uchiyama, S.; Kato, K.; Fujita, M. *Nat. Commun.* **2012**, *3*, 1093.

(2) For recent examples, see, e.g.: (a) Sun, Q. F.; Iwasa, J.; Ogawa, D.; Ishido, Y.; Sato, S.; Ozeki, T.; Sei, Y.; Yamaguchi, K.; Fujita, M. *Science* **2010**, *328*, 1144−1147. (b) Freye, S.; Michel, R.; Stalke, D.; Pawliczek, M.; Frauendorf, H.; Clever, G. H. *J. Am. Chem. Soc.* **2013**, *135*, 8476−8479. (c) Riddell, I. A.; Smulders, M. M. J.; Clegg, J. K.; Hristova, Y. R.; Breiner, B.; Thoburn, J. D.; Nitschke, J. R. *Nat. Chem.* **2012**, *4*, 751−756. (d) Alberti, F. M.; Zielinski, W.; Morell Cerda, M.; Sanz Miguel, P. J.; Troeppner, O.; Ivanovic-Burmazovic, I.; Lippert, B. *Chem.—Eur. J.* **2013**, *19*, 9800−9806. (e) Zheng, Y.-R.; Lan, W.-J.; Wang, M.; Cook, T. R.; Stang, P. J. *J. Am. Chem. Soc.* **2011**, *133*, 17045−17055. (f) Osuga, T.; Murase, T.; Fujita, M. *Angew. Chem., Int. Ed.* **2012**, *124*, 12199−12201. (g) Clever, G. H.; Kawamura, W.; Tashiro, S.; Shiro, M.; Shionoya, M. *Angew. Chem., Int. Ed.* **2012**, *51*, 2606−2609. (h) Frank, M.; Hey, J.; Balcioglu, I.; Chen, Y.-S.; Stalke, D.; Suenobu, T.; Fukuzumi, S.; Frauendorf, H.; Clever, G. H. *Angew. Chem., Int. Ed.* **2013**, *52*, 10102−10106.

(3) See, e.g.: (a) Yoshizawa, M.; Klosterman, J. K.; Fujita, M. *Angew. Chem., Int. Ed.* **2009**, *48*, 3418−3438 and references therein. (b) Cavarzan, A.; Scarso, A.; Sgarbossa, P.; Strukul, G.; Reek, J. N. H. *J. Am. Chem. Soc.* **2011**, *133*, 2848−2851. (c) Adamala, K.; Szostak, J. W. *Nat. Chem.* **2013**, *5*, 495−501. (d) Sanles-Sobrido, M.; Pérez-Lorenzo, M.; Rodríguez-González, B.; Salgueiriño, V.; Correa-Duarte, M. A. *Angew. Chem., Int. Ed.* **2012**, *51*, 3877−3882. (e) Borsato, G.; Scarso, A. In *Selective Nanocatalysis and Nanoscience*; Zecchina, A., Bordiga, S., Groppo, E., Eds.; Wiley-VCH: Weinheim, 2011; pp 105−168 and references therein. (f) Russell, J. T.; Lin, Y.; Böker, A.; Su, L.; Carl, P.; Zettl, H.; He, J.; Sill, K.; Tangirala, R.; Emrick, T.; Littrell, K.; Thiyagarajan, P.; Cookson, D.; Fery, A.; Wang, Q.; Russell, T. P. *Angew. Chem., Int. Ed.* **2005**, *44*, 2420−2426.

(4) See, e.g.: (a) Boekhoven, L.; Pérez, C. M. R.; Sur, S.; Worthy, A.; Stupp, S. I. *Angew. Chem., Int. Ed.* **2013**, *52*, 12077−1208. (b) An, Q.; Brinkmann, J.; Huskens, J.; Krabbenborg, S.; de Boer, J.; Jonkheijm, P. *Angew. Chem., Int. Ed.* **2012**, *51*, 12233−12237.

(5) See, e.g.: (a) Douglas, T.; Young, M. *Nature* **1998**, *393*, 152−155. (b) Muñoz, B.; Rámila, A.; Pérez-Pariente, J.; Díaz, I.; Vallet-Regí, M. *Chem. Mater.* **2003**, *15*, 500−503. (c) Zhang, J.; Sun, H.; Ma, P. X. *ACS Nano* **2010**, *4*, 1049−1059. (d) Xu, C.; Lin, Y.; Wang, J.; Wu, L.; Wei, W.; Ren, J.; Qu, X. *Adv. Healthcare Mater.* **2013**, *2*, 1591−1599. (e) Zhang, J.; Sun, H.; Ma, P. X. *ACS Nano* **2010**, *4*, 1049−1059. (f) Li, C.; Luo, G.-F.; Wang, H.-Y.; Zhang, J.; Gong, Y.-H.; Cheng, S.-X.; Zhuo, R.-X.; Zhang, X.-Z. *J. Phys. Chem. C* **2011**, *115*, 17651−17659.

(6) See, e.g.: (a) Galstyan, A.; Sanz Miguel, P. J.; Lippert, B. *Chem.—Eur. J.* **2010**, *16*, 5577−5780. (b) Galstyan, A.; Sanz Miguel, P. J.; Lippert, B. *Dalton Trans.* **2010**, *39*, 6386−6388. (c) Galstyan, A.; Shen, W.-Z.; Freisinger, E.; Alkam, H.; Hiller, W.; Sanz Miguel, P. J.; Schürmann, M.; Lippert, B. *Chem.—Eur. J.* **2011**, *17*, 10771−10780. (d) Ibáñez, S.; Albertí, F. M.; Sanz Miguel, P. J.; Lippert, B. *Chem.—Eur. J.* **2011**, *17*, 9283−9287. (e) Galstyan, A.; Sanz Miguel, P. J.; Weise, K.; Lippert, B. *Dalton Trans.* **2013**, *42*, 16151−16161.

(7) See, e.g.: (a) Suntharalingam, K.; Gupta, D.; Sanz Miguel, P. J.; Lippert, B.; Vilar, R. *Chem.—Eur. J.* **2010**, *16*, 3613−3616. (b) von Grebe, P.; Suntharalingam, K.; Vilar, R.; Sanz Miguel, P. J.; Herres-Pawlis, S.; Lippert, B. *Chem.—Eur. J.* **2013**, *19*, 11429−11438. (c) Albertí, F. M.; Rodríguez-Santiago, L.; Sodupe, M.; Mirats, A.; Kaitsiotou, H.; Sanz Miguel, P. J.; Lippert, B. *Chem.—Eur. J.* **2014**, *20*, 3394−3407.

(8) See, e.g.: (a) Kampf, G.; Sanz Miguel, P. J.; Morell Cerda, M.; Willermann, M.; Schneider, A.; Lippert, B. *Chem.—Eur. J.* **2008**, *14*, 6882−6891. (b) Yin, L.; Sanz Miguel, P. J.; Shen, W.-Z.; Lippert, B. *Chem.—Eur. J.* **2009**, *15*, 10723−10726. (c) Brandi-Blanco, P.; Sanz Miguel, P. J.; Lippert, B. *Eur. J. Inorg. Chem.* **2012**, 1122−1129. (d) Yin, L.; Sanz Miguel, P. J.; Hiller, W.; Lippert, B. *Inorg. Chem.* **2012**, *51*, 6784−6793. (e) Holland, L.; Shen, W.-Z.; von Grebe, P.; Sanz Miguel, P. J.; Pichierri, F.; Springer, A.; Schalley, C. A.; Lippert, B. *Dalton Trans.* **2011**, *40*, 5159−5161.

(9) For Ag−NHC constructs, see: (a) Hahn, F. E.; Jahnke, M. C. *Angew. Chem., Int. Ed.* **2008**, *47*, 3122−3172. (b) Rit, A.; Pape, T.; Hahn, F. E. *J. Am. Chem. Soc.* **2010**, *32*, 4572−4573. (c) Hahn, F. E.; Radloff, C.; Pape, T.; Hepp, A. *Organometallics* **2008**, *27*, 6408−6410. (d) Conrady, F. M.; Fröhlich, R.; to Brinke, C. S.; Pape, T.; Hahn, F. E. *J. Am. Chem. Soc.* **2011**, *133*, 11496−11499. (e) Hahn, F. E.; Radloff, C.; Pape, T.; Hepp, A. *Chem.—Eur. J.* **2008**, *14*, 10900−10904. (f) Rit, A.; Pape, T.; Hahn, F. E. *Organometallics* **2011**, *30*, 6393−6401. (g) Han, Y.-F.; Jin, G.-X.; Hahn, F. E. *J. Am. Chem. Soc.*

2013, *135*, 9263−9266. (h) Schmidtendorf, M.; Pape, T.; Hahn, F. E. *Angew. Chem., Int. Ed.* **2012**, *51*, 2238−2242.
(10) (a) Wang, H. M. J.; Lin, I. J. B. *Organometallics* **1998**, *17*, 972−975. (b) Garrison, J. C.; Youngs, W. J. *Chem. Rev.* **2005**, *105*, 3978−4008. (c) Ku, R.-Z.; Huang, J.-C.; Cho, J.-Y.; Kiang, F.-M.; Reddy, K. R.; Chen, Y.-C.; Lee, K.-J.; Lee, J.-H.; Lee, G.-H.; Peng, S.-M.; Liu, S.-T. *Organometallics* **1999**, *18*, 2145−2154.
(11) For Au mechanisms, see, e.g.: (a) Brooner, R. E. M.; Brown, T. J.; Widenhoefer, R. A. *Angew. Chem., Int. Ed.* **2013**, *52*, 6259−6261. (b) Seidel, G.; Gabor, B.; Goddard, R.; Heggen, B.; Thiel, W.; Fürstner, A. *Angew. Chem., Int. Ed.* **2014**, *53*, 879−882.
(12) (a) Iglesias, M.; Pérez-Nicolás, M.; Sanz Miguel, P. J.; Polo, V.; Fernández-Alvarez, F. J.; Pérez-Torrente, J. J.; Oro, L. A. *Chem. Commun.* **2012**, *48*, 9480−9482. (b) Iglesias, M.; Sanz Miguel, P. J.; Polo, V.; Fernandez-Alvarez, F. J.; Pérez-Torrente, J. J.; Oro, L. A. *Chem.—Eur. J.* **2013**, *19*, 17559−17566.
(13) See, e.g.: (a) Zhang, J.-P.; Wang, Y.-B.; Huang, X.-C.; Lin, Y.-Y.; Chen, X.-M. *Chem.—Eur. J.* **2005**, *11*, 552−561. (b) Scherbaum, F.; Grohmann, A.; Huber, B.; Krüger, C.; Schmidbaur, H. *Angew. Chem.* **1988**, *100*, 1602−1604. (c) Goodwin, A. L.; Keen, D. A.; Tucker, M. G.; Dove, M. T.; Peters, L.; Evans, J. S. O. *J. Am. Chem. Soc.* **2008**, *130*, 9660−9661. (d) Mohamed, A. A.; Pérez, L. M.; Fackler, J. P., Jr. *Inorg. Chim. Acta* **2008**, *358*, 1657−1662. (e) Yang, G.; Baran, P.; Martínez, A. R.; Raptis, R. G. *Cryst. Growth Des.* **2013**, *13*, 264−269. (f) Meyer, F.; Jacobi, A.; Zsolnai, L. *Chem. Ber./Recl.* **1997**, *130*, 1441−1447. (g) Krishantha, D. M. M.; Gamage, C. S. P.; Schelly, Z. A.; Dias, H. V. R. *Inorg. Chem.* **2008**, *47*, 7065−7067.
(14) *APEX2*; Bruker AXS Inc.: Madison, WI, 2011.
(15) Sheldrick, G. M. *SHELXS-97 and SHELXL-97*; University of Göttingen: Göttingen, Germany, 1997.
(16) Farrugia, L. J. *WinGX*; University of Glasgow: Glasgow, United Kingdom, 1998.
(17) (a) Zhao, Y.; Truhlar, D. G. *Theor. Chem. Acc.* **2008**, *120*, 215−241. (b) Zhao, Y.; Truhlar, D. G. *Acc. Chem. Res.* **2008**, *41*, 157−167. (c) Zhao, Y.; Truhlar, D. G. *J. Chem. Phys.* **2006**, *125*, 194101−194118.
(18) (a) Becke, A. D. *J. Chem. Phys.* **1993**, *98*, 5648−5652. (b) Lee, C.; Yang, W.; Parr, R. G. *Phys. Rev. B* **1988**, *37*, 785−789. (c) Stephens, P. J.; Devlin, F. J.; Chabalowski, C. F.; Frisch, M. J. *J. Phys. Chem.* **1994**, *98*, 11623−11627.
(19) Marenich, A. V.; Cramer, C. J.; Truhlar, D. G. *J. Phys. Chem. B* **2009**, *113*, 6378−6396.
(20) (a) Andrae, D.; Haussermann, U.; Dolg, M.; Stoll, H.; Preuss, H. *Theor. Chim. Acta* **1990**, *77*, 123−141. (b) Dolg, M.; Stoll, H.; Preuss, H.; Pitzer, R. M. *J. Phys. Chem.* **1993**, *97*, 5852−5859.
(21) Frisch, M. J.; Trucks, G. W.; Schlegel, H. B.; Scuseria, G. E.; Robb, M. A.; Cheeseman, J. R.; Montgomery, J. A., Jr.; Vreven, T.; Kudin, K. N.; Burant, J. C.; Millam, J. M.; Iyengar, S. S.; Tomasi, J.; Barone, V.; Mennucci, B.; Cossi, M.; Scalmani, G.; Rega, N.; Petersson, G. A.; Nakatsuji, H.; Hada, M.; Ehara, M.; Toyota, K.; Fukuda, R.; Hasegawa, J.; Ishida, M.; Nakajima, T.; Honda, Y.; Kitao, O.; Nakai, H.; Klene, M.; Li, X.; Knox, J. E.; Hratchian, H. P.; Cross, J. B.; Adamo, C.; Jaramillo, J.; Gomperts, R.; Stratmann, R. E.; Yazyev, O.; Austin, A. J.; Cammi, R.; Pomelli, C.; Ochterski, J. W.; Ayala, P. Y.; Morokuma, K.; Voth, G. A.; Salvador, P.; Dannenberg, J. J.; Zakrzewski, V. G.; Dapprich, S.; Daniels, A. D.; Strain, M. C.; Farkas, O.; Malick, D. K.; Rabuck, A. D.; Raghavachari, K.; Foresman, J. B.; Ortiz, J. V.; Cui, Q.; Baboul, A. G.; Clifford, S.; Cioslowski, J.; Stefanov, B. B.; Liu, G.; Liashenko, A.; Piskorz, P.; Komaromi, I.; Martin, R. L.; Fox, D. J.; Keith, T.; Al-Laham, M. A.; Peng, C. Y.; Nanayakkara, A.; Challacombe, M.; Gill, P. M. W.; Johnson, B.; Chen, W.; Wong, M. W.; Gonzalez, C.; Pople, J. A. *Gaussian 09*, Rev. B.04; Gaussian Inc.: Pittsburgh, PA, 2009.